Available online at www.sciencedirect.com
ScienceDirect
Ceramics International 36 (2010) 2395–2400
CERAMICS INTERNATIONAL
www.elsevier.com/locate/ceramint

Effect of cesium substitution on the thermal evolution and ceramics formation of potassium-based geopolymer

Peigang He, Dechang Jia *, Meirong Wang, Yu Zhou

Institute for Advanced Ceramics, Harbin Institute of Technology, Harbin 150080, China

Received 26 April 2010; received in revised form 15 May 2010; accepted 14 June 2010
Available online 3 August 2010

Abstract

The thermal evolution of cesium-substituted potassium-based geopolymer ($(K_{1-x}Cs_x)_2O{\cdot}Al_2O_3{\cdot}5SiO_2{\cdot}11H_2O$, $x = 0$, 0.1, 0.2, 0.3, and 0.4) on heating is studied by a variety of techniques. Phase compositions and thermal expansion behaviors of the ceramics derived from the geopolymer are characterized. All of the geopolymer specimens with or without cesium substitution exhibit similar thermal evolution trends. Major weight losses before 600 °C from all the geopolymer specimens are observed and are resulted from evaporation of free water and hydroxyl groups. Thermal shrinkage of these specimens can be divided into four stages, i.e. structural resilience, dehydration, dehydroxylation and sintering, according to the dilatometer results. For these specimens, significant difference is observed in the viscous sintering stage and the effect of cesium is to reduce the thermal shrinkage in this stage due to the increased matrix viscosity. In the ceramics derived from geopolymer, the amount of stabilized leucite increases with the amount of cesium and with 20% cesium substitution leucite is fully stabilized in cubic phase.

Keywords: C. Thermal expansion; Microstructure; Geopolymer

1. Introduction

In recent years geopolymer materials have attracted a lot of attention for their excellent fire resistance, low cost, environmentally friendly nature and excellent thermal properties [1–5]. Most importantly, geopolymer technology provides a new method to fabricate leucite ceramics [6–13]. As compared with sol–gel and hydrothermal methods, geopolymer technology is advantageous in low cost and short fabricating time and with the proper processing procedure geopolymer can be directly converted into the final structural ceramic part of interest. Meanwhile, because geopolymer is typically made by mixing an aluminosilicate source into an alkaline silicate solution, it is convenient to design the chemical composition of the final products.

On the other hand, leucite undergoes a rapid and reversible displacive phase transition from tetragonal to cubic symmetry between 400 and 600 °C, accompanied by a large volume increase of ~1.2% [14,15]. The overall volume increase of the unit cell is associated with a change in the thermal expansion coefficient (CTE) from 22.3×10^{-6}/°C over the range from 25 to 400 °C to 21.5×10^{-6}/°C over the range of 400–700 °C [14]. The structural transformation and high CTE during thermal cycling will result in microcracking of the leucite matrix and high volume instability, which are detrimental to its widespread use like composites. In order to inhibit the phase transformation, some works have been done. Researchers find that cubic leucite can be stabilized at room temperature by the addition of cesium carbonate [16] or pollucite [17] to the starting composition. Meanwhile, the thermal expansion of the stabilized cubic leucite can also be tailored by using cesium.

Our preliminary exploratory investigation has proved that with 40% cesium substitution for potassium, leucite derived from Cs–K-based geopolymer could be stabilized in cubic form at room temperature and coefficient of thermal expansion of the resulted ceramic decreases dramatically. Therefore, the Cs–K-based geopolymer may provide a new precursor to fabricate ceramics which can be used in ceramic matrix composites, thermal-shock resistant molds, and refractory areas. However, until now the thermal evolution and crystallization of Cs–K-based geopolymer has not been explored.

* Corresponding author at: P.O. Box 3022, No. 2 Yikuang Street, Institute for Advanced Ceramics, HIT Science Park, Harbin Institute of Technology, Harbin 150080, PR China. Tel.: +86 451 86418792; fax: +86 451 86414291.
E-mail address: dcjia@hit.edu.cn (D. Jia).

0272-8842/$36.00.
doi:10.1016/j.ceramint.2010.07.015

In this paper, mixed alkaline silicate solutions are used to fabricate cesium-substituted potassium-based geopolymer with nominal composition of $(K_{1-x}Cs_x)_2O{\cdot}Al_2O_3{\cdot}5SiO_2{\cdot}11H_2O$ (referred to as $(K_{1-x}Cs_x)$GP, $x = 0$, 0.1, 0.2, 0.3, and 0.4). Because geopolymer with higher cesium content is much more difficult to densify upon heating than that with lower cesium content [7,8], it can be inferred that with increasing cesium content, onset temperature for sintering stage of Cs–K-based geopolymer would increase gradually, which might lead to the volatization of cesium [8]. Meanwhile, cesium hydroxide (CsOH) is much more expensive than potassium hydroxide (KOH). Thus, in our investigation the cesium substitution amount for potassium is limited to 40% based on the preliminary exploratory investigation. The aims of this study are (1) to measure the effects of cesium substitution on the thermal evolution of geopolymer; (2) to investigate the role of Cs^+ substitution for K^+ ions on stabilizing the high-temperature form of leucite and thermal expansion properties of the ceramic derived from geopolymer. Relevant studies are rarely reported before.

2. Experimental procedures

$(K_{1-x}Cs_x)$GP with composition of $SiO_2/Al_2O_3 = 5$, $R_2O/SiO_2 = 0.2$ and $H_2O/R_2O = 11$ (mole ratio) were obtained by mixing metakaolin with alkaline silicate solutions. These ratios were chosen based on our previous work, as it allowed for optimal mechanical and thermal properties. Alkaline silicate solution based on five differing ratios of alkali metal Cs/(Cs + K) = (0, 0.1, 0.2, 0.3, and 0.4) were prepared by dissolving amorphous silica (Shanghai Dixiang Indus, China) into a mixed KOH (Tianjin Fuchen Indus., China) and CsOH (Jiangxi Dongpeng New Materials Co., Ltd.) solution. The solution was then allowed to mature under stirring for 48 h in order to dissolve the silica completely. The main phase of metakaolin (800 °C calcined Kaolin, Shanghai Fengxian Indus., China) was amorphous with a characteristic hump centered at about 23° in 2θ and its minor phase was quartz. The resultant slurries were cast into polystyrene containers (70 mm in diameter and 80 mm in height), sealed, and cured at 70 °C for 48 h. After demoulding the hardened $(K_{1-x}Cs_x)$GPs were further cured at 70 °C for 24 h.

Simultaneous TGA and DTA (Netzsh STA 409, Germany) were carried out at 5 °C/min in an atmosphere of flowing Ar (20 ml/min) in alumina crucibles over a temperature range from 35 to 1200 °C. The linear thermal expansion behavior of $(K_{1-x}Cs_x)$GP from 30 to 1250 °C was determined with a high–temperature dilatometer (Netzsch DIL 402C, Germany) at 5 °C/min in an Ar gas atmosphere, and the data were corrected using the known thermal expansion of a certified standard carbon. The final dimension of the sample was approximately 4 mm × 4 mm × 20 mm, and was carefully polished before thermal expansion measurement. A scanning electron microscope (SEM: FEI Quanta 200F, Eindhoven, The Netherlands) was used to observe the fractograph of geopolymer before and after heat treatment.

The phases of samples after heating to 1200 °C at 5 °C/min for 3 h soak were characterized by an X-ray diffractometer (XRD: Rigaku, D/MAX-2200VPC, Tokyo, Japan) with CuKα radiation. Continuous scans were used for qualitative phase identification at a scan rate of 4°/min, while slow step scans with a step width of 0.02° and a step time of 3 s were carried out to determine the shifts of X-ray spectrum, and hence calculate the lattice parameters of ceramics.

3. Results and discussion

3.1. Thermal evolution of $(K_{1-x}Cs_x)$GP

3.1.1. TG/DTA analysis

The thermal gravimetry (TG) results of $(K_{1-x}Cs_x)$GP upon heating are presented in Fig. 1. It can be observed that all specimens exhibited similar characteristic trends up to 1300 °C. A significant weight loss was observed from room temperature (RT) to 300 °C in each TG curve. It resulted from the evaporation of free water including unconstrained surface water and pore water in $(K_{1-x}Cs_x)$GP. With increasing Cs content, the mass loss in this temperature range decreased regularly, which might be related to the relative amount of hydration water associated with the Cs and K. For the decreased energy of hydration of $Cs^+_{(aq)}$ compared to $K^+_{(aq)}$ [18], the amount of hydration water associated with the Cs was much lower than that with K, so during continuous heating the mass loss decreased gradually with Cs content. Over the range from 300 to 600 °C, there was another weight loss which was attributed to the liberation of water by condensation/polymerization of Si–OH and Al–OH groups [8–10]. When temperature further increased, KGP exhibited little weight change. However, $(K_{1-x}Cs_x)$GP ($0 < x \leq 0.4$) showed another slow weight loss stage and it was more obvious for specimens with $x > 0.2$. The weight loss at this temperature range might be due to cesium volatization. Because metakaolin was only partially dissolved in geopolymer (as shown in Section 3.1.3), not all of the alkali cations were bound within the geopolymer structure. Moreover, it had been reported that cesium can be easily volatilized from pollucite or analcime at temperature above 1000 °C [19]. Therefore, on heating, the free cesium was easily volatilized, leading to the weight loss.

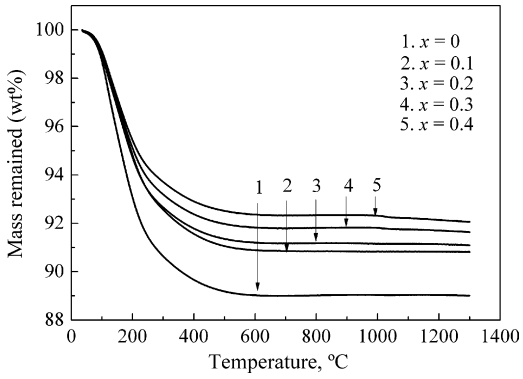

Fig. 1. Weight loss of the as-prepared geopolymer specimens of $(K_{1-x}Cs_x)$GP measured by TGA from RT to 1300 °C.

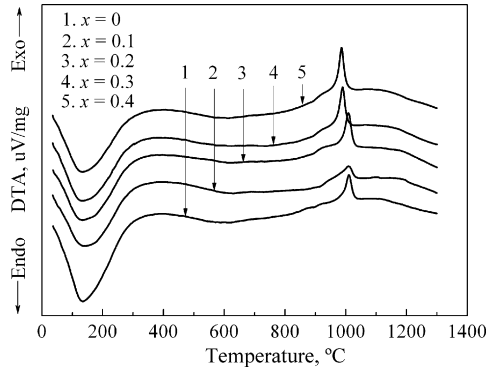

Fig. 2. DTA thermograms of the as-prepared geopolymer specimens of $(K_{1-x}Cs_x)$GP from RT to 1300 °C. The offset in the DTA curves are introduced for display purposes.

All specimens also exhibit similar DTA thermograms, as shown in Fig. 2. Two characteristic features were observed from each thermogram: a large endothermic peak at low temperature region and a sharp exothermic peak at high temperature region. The large endothermic peaks in the DTA curves extended from 35 to 300 °C and were attributed to the evaporation of free water in geopolymer, as indicated in thermogravimetric analysis. At the high temperature region the exothermic peaks were caused by leucite crystallization, which had been demonstrated in our recent study. With increasing cesium content from 0 to 0.4, the exothermic peaks gradually shifted to lower temperatures, i.e. from 1010.3 to 986.3 °C. Bell et al. [7,8] respectively observed an exotherm due to leucite and pollucite crystallization from potassium- and cesium-based geopolymer. In unheated cesium-based geopolymer there were many small nuclei which served as the crystallization site for the crystallization. Therefore, as compared with potassium-based geopolymer, on heating cesium-based geopolymer would crystallize at a lower temperature. With increasing cesium content, the number of nucleus would increase gradually accounting for the measured results in this study.

3.1.2. Dilatometry analysis

Fig. 3 illustrates the variations in the thermal shrinkage of the $(K_{1-x}Cs_x)$GP ($x = 0$, 0.1, 0.2, 0.3, and 0.4) with correction. All specimens exhibited four thermal shrinkage stages, named as (I) structural resilience, (II) dehydration, (III) dehydroxylation and (IV) sintering stage. They were consistent with the observation in a variety of geopolymer, regardless of alkali choice (Cs, K, and Na) or Si/Al ratio [7–10].

(1) Stage I extended from approximately 25 to ∼ 100 °C. Minimal shrinkage was observed in all specimens as only free water from large pores and surfaces was lost in this stage.
(2) Stage II was over the range of 100 to ∼300 °C, and involved initial stage of rapid thermal shrinkage. Shrinkage in this stage was due to capillary contraction created when water was evaporated from the micro- and nano-pores of $(K_{1-x}Cs_x)$GP.
(3) Stage III occurred over a temperature range from 300 to 700–900 °C. The shrinkage in this stage resulted from the physical contraction of $(K_{1-x}Cs_x)$GP during condensation reaction from T–OH groups to T–O–T linkages.
(4) Stage IV displayed a significant thermal shrinkage, which was due to both skeletal densification and elimination of large pores by viscous sintering. Large differences in this stage were observed between these specimens.

In viscous flow sintering, atomic movement occurred by a cooperative motion mechanism rather than individual diffusion, and this had been well studied in glasses and sol–gel materials [20]. The onset temperature of stage IV occurred approximately at 700, 850, 865, 870 and 900 °C for specimens with $x = 0$, 0.1, 0.2, 0.3, and 0.4, respectively. It indicated that geopolymers with higher cesium content were more refractory than those with lower cesium content. Bell et al. [7] reported that cesium-based geopolymer was much more refractory compared with potassium- and sodium-based geopolymer and viscous sintering did not occur until the sample was heated to above 1200 °C. On the other hand, no eutectic melts with similar composition of $K_{(1-0.7)}Cs_{(0-0.4)}AlSi_2O_6$ were found in the quaternary Cs_2O–K_2O–Al_2O_3–SiO_2 system [19]. Thus with increasing cesium content, the viscosity of the geopolymer gel increased, leading to the increased onset sintering temperature. It was also apparent from Fig. 3 that with increasing cesium content specimens underwent a decreased magnitude of densification, implying that the barrier to densification was increased greatly in the presence of cesium, correlating with the increase in viscosity. The increase in viscosity of geopolymer gel was likely to be the result of leucite crystallization. Based on the aforementioned DTA analysis, the crystallization peak temperature decreased as the x increase for $0 \leq x \leq 0.4$, from 1010.3 to 1009.7, 1009.0, 989.8 and 986.3 °C, respectively and stage IV extended temperature ranges of 700–954.3, 850–993.7, 865–1004.4, 870–997.3 and 900–1008.5 °C for specimens with $x = 0$, 0.1, 0.2, 0.3, and 0.4, respectively. Crystallization peak temperatures for specimens with $x < 0.3$ were higher than the end temperatures of their respective stage IV. It means that before specimens was fully densified there was no (for $x = 0$) or only a small amount of leucite formed (for $x = 0.1$, 0.2), which was beneficial for the sintering densification of the specimens. However, for those with $x \geq 0.3$, crystallization occurred in the stage IV of thermal shrinkage, which would undoubtedly raise

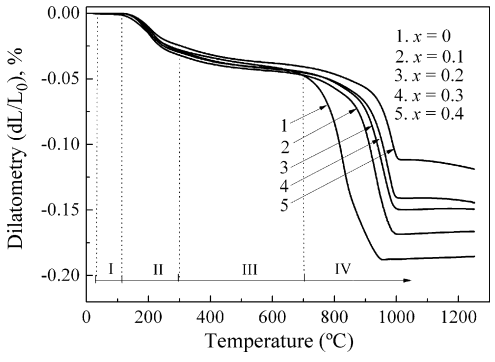

Fig. 3. Thermal shrinkage of the as-prepared geopolymer specimens of $(K_{1-x}Cs_x)$GP from RT to 1300 °C.

the viscosity of the matrix and slow down the sintering rate [21] and further sintering would proceed at a higher temperature, as observed in the tails of the $(K_{0.7}Cs_{0.3})$GP and $(K_{0.6}Cs_{0.4})$GP.

3.1.3. SEM observation

Fig. 4 shows typical microstructure of $(K_{1-x}Cs_x)$GP ($x = 0$, 0.3) before and after heat treatment at 1200 °C for 3 h in Ar. Microstructures were not significantly different between the geopolymers with and without cesium substitution. The structure of unheated geopolymers contained partially reacted metakaolin (Fig. 4(a) and (b)) and the binder phase of geopolymer consisted of fine nanometer precipitates (Fig. 4(c) and (d)). After being heated to 1200 °C, these precipitates coarsened substantially and both geopolymers develop a smooth, glassy texture (Fig. 4(e) and (f)). The coarsening was consistent with the large amount of shrinkage observed over the sintering temperature range. Closed pores were also observed which were created during the significant coarsening and surface area reduction.

3.2. Characterization of $(K_{1-x}Cs_x)$GP ceramics

3.2.1. Phase composition of $(K_{1-x}Cs_x)$GP ceramics

Fig. 5 graphically displays the XRD analyses of $(K_{1-x}Cs_x)$GP after being treated at 1200 °C for 3 h soak at 5 °C/min in Ar. The XRD results showed that the Cs^+ substitution for K^+ ions successfully stabilized the high-temperature cubic form of leucite. Cubic leucite stabilization was best characterized by following the evolution of typical diffraction peaks at the 2θ value of about 25.9° (0 0 4) and 27.3° (4 0 0) of tetragonal leucite and 26.3° (4 0 0) of cubic leucite. Tetragonal leucite was the only crystalline phase present in

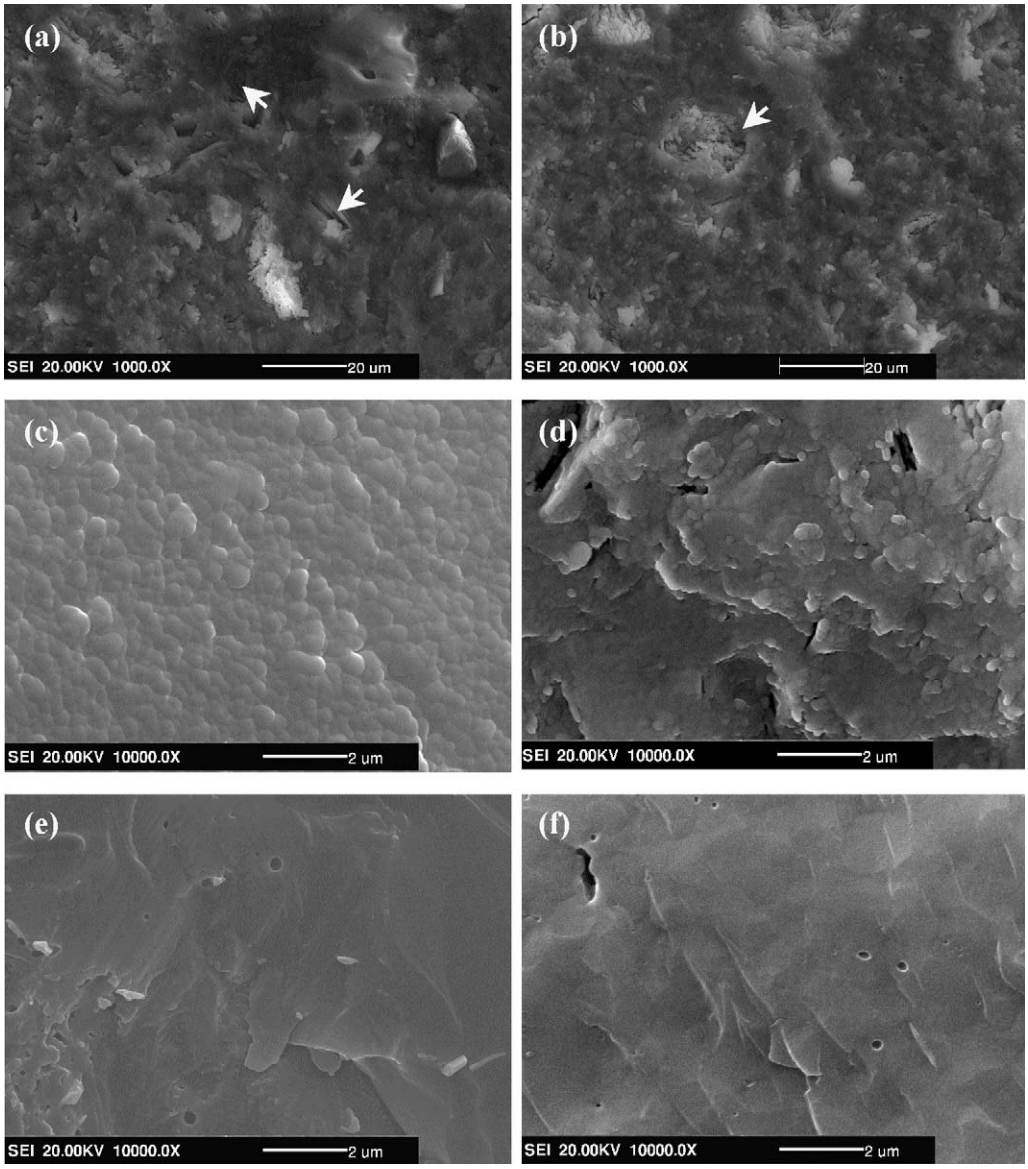

Fig. 4. Microstructure of $(K_{1-x}Cs_x)$GP before and after heat treatment at 1200 °C for 3 h: (a), (c) and (e) $x = 0$; (b), (d) and (f) $x = 0.3$. The write arrows indicate the partially reacted metakaolin.

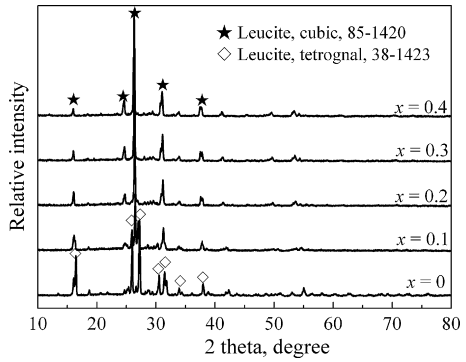

Fig. 5. X-ray diffraction patterns of $(K_{1-x}Cs_x)$GP ceramics. The offsets in the XRD curves are introduced for display purposes. The samples were prepared by heating the as-prepared geopolymers at 1200 °C for 3 h soak at 5 °C/min in Ar.

KGP ($x = 0$). A small amount of cubic leucite was found after 10% Cs^+ ions substituting for K^+ ions ($x = 0.1$). The intensity of (4 0 0) peak ($2\theta \approx 26.3^\circ$) increased with the increment of Cs content, which indicated the amount of stabilized cubic leucite increased and with 20% cesium substitution ($x = 0.2$), leucite was fully stabilized in cubic phase. No detectable amount of pollucite was observed in all of the samples.

Taylor [22] and Naray-Szabo [23] had reported that K^+ and Cs^+ ions occupied the same crystallographic sites (W sites) in both leucite and pollucite structures. The crystal structure of pollucite ($CsAlSi_2O_6$) was cubic at room temperature. Compared with the cesium ion, the smaller size of the potassium ion (1.66 Å vs. 1.88 Å) kept it from filling the W sites completely, leading to a lattice deformation from cubic to tetragonal through the twisting of the tetrahedral framework around [0 0 1] [17]. In the original geopolymer, Cs was located in similar cation sites to the K. For $(K_{1-x}Cs_x)$GP, some of the potassium ions were replaced with cesium ions. With increasing cesium content, the average radius of alkali metal ion increased gradually. So, during the soak at 1200 °C the mixed ions can fill the W site much more completely than the single K and when the cesium-substituted leucite was cooled down, lattice deformation could be prevented and the high-temperature cubic structure was stabilized as a result.

Fig. 6(a) shows the XRD patterns of $(K_{1-x}Cs_x)$GP ceramics in a 2θ range of 24.5–28°. The peak (4 0 0) of cubic leucite for $(K_{1-x}Cs_x)$GP ceramics shifted gradually toward the low angle region with the increase of x from $(K_{0.9}Cs_{0.1})$GP ($x = 0.1$) to $(K_{0.6}Cs_{0.4})$GP ($x = 0.4$), which was directly related to the change in average ionic radius from K^+ (1.64 Å) to Cs^+ (1.88 Å). The lattice parameters calculated as a function of the content of Cs are depicted in Fig. 6(b). The lattice parameters exhibited an approximate linear increase with increasing cesium content from $x = 0.1$ to $x = 0.4$, which strongly implied the progressive inclusion of cesium ions in place of potassium ions in the large W sites of the leucite framework.

3.2.2. Thermal expansion properties of $(K_{1-x}Cs_x)$GP ceramics

The results of the dilatometric measurement for $(K_{1-x}Cs_x)$GP ceramics ($x = 0$, 0.1, 0.2, 0.3, 0.4) with correction are shown in

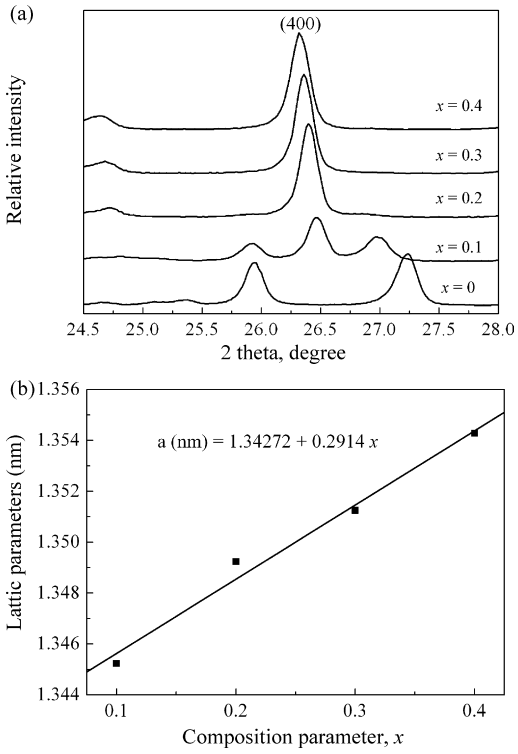

Fig. 6. Slow step-scan XRD patterns and the calculated lattice parameters of $(K_{1-x}Cs_x)$GP ceramics: (a) the (4 0 0) peak in a 2θ range of 24.5–28, and (b) lattice parameters.

Fig. 7. The thermal expansion of the ceramics increased with the increase of temperature, which was attributed to the increasing atomic spacing at elevated temperatures. Clearly, KGP ($x = 0$) exhibited an abrupt large volume change in temperature range of 410–470 °C due to the tetragonal to cubic leucite transformation. In contrast, no abrupt volume change was observed for $(K_{1-x}Cs_x)$GP ceramics ($x \geq 0.2$) from 30 to 1300 °C, implying cubic leucite was fully stabilized.

The average thermal expansion coefficient is defined as the average value of the relative length change in the temperature range of $T_1 < T < T_2$, as described by the following equation (1):

$$\alpha_a = \frac{L_2 - L_1}{L_0(T_2 - T_1)} = \frac{\Delta L}{L_0\,\Delta T} \quad (1)$$

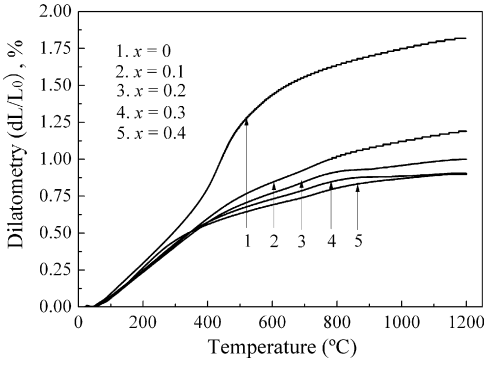

Fig. 7. Linear coefficient of thermal expansion of $(K_{1-x}Cs_x)$GP ceramic. The samples were prepared by the same method as depicted in Fig. 5.

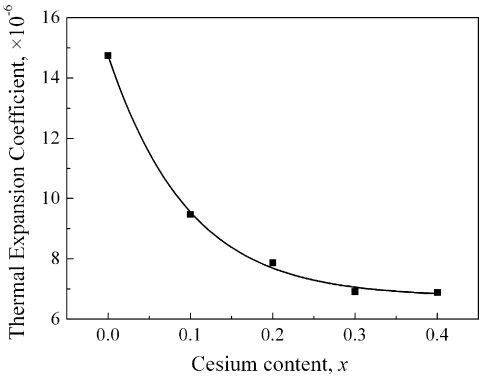

Fig. 8. The average thermal expansion coefficients of $(K_{1-x}Cs_x)$GP ceramics in the temperature range of 30–1300 °C.

where L_0, L_1, and L_2 are the lengths of the specimen at temperatures of T_0 (30 °C), T_1, and T_2, respectively. The average thermal expansion coefficients of $(K_{1-x}Cs_x)$GP in the temperature range of 30–1300 °C are shown in Fig. 8. It was clearly seen that the average thermal expansion coefficients of $(K_{1-x}Cs_x)$GP ceramics decreased exponentially from 14.74 ($x = 0$) to 6.89 ($x = 0.4$) with increase in cesium substitution in the temperature range of 30–1300 °C, which mainly resulted from the increased stabilized cubic leucite content in the ceramics.

4. Conclusions

The following conclusions are drawn from the investigation presented in this paper:

(1) All cesium-substituted potassium-based geopolymer specimens exhibit similar thermal evolution trend and it can be divided into four characteristic stages of structural resilience, dehydration, dehydroxylation and sintering. The extent of thermal shrinkage observed in the sintering stage of geopolymers decreases rapidly for cesium content, i.e. $0 \leq x \leq 0.4$, which is due to the increased matrix viscosity.
(2) The cesium substitution for potassium was effective in stabilizing the cubic polymorph of leucite to room temperature and with 20% cesium substitution leucite was completely stabilized into cubic phase. As increasing the cesium substitution, the average thermal expansion coefficients of the $(K_{1-x}Cs_x)$GP ceramics decrease exponentially.

Acknowledgements

This work was supported by Program for New Century Excellent Talents in University (NCET, Grant No. NCET-04-0327), Program of Excellent Team in Harbin Institute of Technology and the Science Fund for Distinguished Young Scholars of Heilongjiang Province.

References

[1] J. Davidovits, Geopolymer—inorganic polymeric new materials, J. Therm. Anal. 37 (8) (1991) 1633–1656.
[2] J. Davidovits, 30 years of successes and failures in geopolymer applications, in: Geopolymer Conference, Melbourne, Australia, 2002.
[3] J. Davidovits, M. Davidovics, Geopolymer: ultra-high temperature tooling material for the manufacture of advanced composites, SAMPE 36 (2) (1991) 1939–1949.
[4] V.F.F. Barbosa, K.J.D. MacKenzie, Thermal behaviour of inorganic geopolymers and composites derived from sodium polysialate, Mater. Res. Bull. 38 (2) (2003) 319–331.
[5] M. Schmücker, K.J.D. MacKenzie, Microstructure of sodium polysialate siloxo geopolymer, Ceram. Int. 31 (2005) 433–437.
[6] V.F.F. Barbosa, K.J.D. MacKenzie, Synthesis and thermal behaviour of potassium sialate geopolymers, Mater. Lett. 57 (9–10) (2003) 1477–1482.
[7] J.L. Bell, P.E. Driemeyer, W.M. Kriven, Formation of ceramics from metakaolin-based geopolymers. Part I. Cs-based geopolymer, J. Am. Ceram. Soc. 92 (1) (2009) 1–8.
[8] J.L. Bell, P.E. Driemeyer, W.M. Kriven, Formation of ceramics from metakaolin-based geopolymers. Part II. K-based geopolymer, J. Am. Ceram. Soc. 92 (3) (2009) 607–615.
[9] P. Duxson, G.C. Lukey, Physical evolution of Na-geopolymer derived from metakaolin up to 1000 °C, J. Mater. Sci. 42 (9) (2007) 3044–3054.
[10] P. Duxson, G.C. Lukey, S.J. Jannie, V. Deventer, The thermal evolution of metakaolin geopolymers. Part 2. Phase stability and structural development, J. Non-Cryst. Solids 353 (22–23) (2007) 2186–2200.
[11] Subaer, A. Riessen, Thermo-mechanical and microstructural characterization of sodium-poly(sialate-siloxo) (Na-PSS) geopolymers, J. Mater. Sci. 42 (9) (2007) 3117–3123.
[12] T. Van Long, Synthesis of nanometer enstatite from precursor gels prepared by the geopolymer technique, Ceram. Int. 34 (2008) 1763–1766.
[13] T. Iwahiro, Y. Nakamura, R. Komatsu, K. Ikeda, Crystallization behavior and characteristics of mullites formed from alumina–silica gels prepared by the geopolymer technique in acidic conditions, J. Eur. Ceram. Soc. 21 (2001) 2515–2519.
[14] D.M. Hatch, S. Ghose, H.T. Stokes, Phase transitions in leucite, $KAlSi_2O_6$, Phys. Chem. Miner. 17 (1990) 220–227.
[15] D.C. Palmer, U. Bismayer, E.K.H. Salje, Phase transition in leucite: order parameter behaviour and the landau potential deduced from Raman spectroscopy and birefringence studies, Phys. Chem. Miner. 17 (1990) 259–265.
[16] T.R. Stephen, L.G. Carole, J.O. William, Stress induced phase transformation of a cesium stabilized leucite porcelain and associated properties, Dent. Mater. 14 (3) (1998) 202–211.
[17] I.L. Denry, J.R. Mackert, J.A. Holloway, S.F. Rosenstiel, Effect of cubic leucite stabilization on the flexural strength of feldspathic dental porcelain, J. Dent. Res. 75 (12) (1996) 1928–1935.
[18] P.A. Kollman, I.D. Kuntz, Studies of cation hydration, J. Am. Ceram. Soc. 94 (26) (1972) 9236–9237.
[19] R.L. Bedard, R.W. Broach, E.M. Flanigen, Leucite-pollucite glass ceramics: a new family of refractory materials with adjustable thermal-expansion, Mater. Res. Soc. Symp. Proc. 271 (1992) 581–587.
[20] A.C. Pierre, Introduction to Sol–Gel Processing, Kluwer Academic, Norwell, MA, 1998.
[21] M.N. Rahaman, L.C. Dejonghe, Effect of rigid inclusions on the sintering of glass powder compacts, J. Am. Ceram. Soc. 70 (12) (1987) C348–C351.
[22] D. Taylor, C.M.B. Henderson, The thermal expansion of the leucite group of minerals, Am. Miner. 53 (1968) 1476–1489.
[23] I. Naray-Szabo, Inorganic Crystal Chemistry, Akademiai Kiado, Budapest, 1969.